Research Article

Signal Pathway Regulation in Mammalian Cells in Wireless Communication Environment

Shengdong Li

College of Life Sciences, Baicheng Normal University, China

Article history
Received: 11-10-2024
Revised: 26-12-2024
Accepted: 06-02-2025

Abstract: To regulate the signal pathway in mammalian cells in a wireless communication environment, an LED light stimulation system has been designed and constructed. To avoid interference from too many data lines, a wireless communication mode has been employed. In this study, HeLa cells and Drosophila melanogaster cells are used as the research objects. The CRY2/CIBN light genetic element system is employed to investigate the regulation of signal protein activity in HeLa cells via the PI3K/Akt signaling pathway and in Drosophila melanogaster cells via the Wnt/β-catenin signaling pathway. This is achieved through the use of an LED light with varying stimulation intensities. The results showed that the level of PI (3,4,5) P3 on the HeLa cell membrane was increased, Akt phosphorylation was enhanced, and the PI3K Signal Pathway in the HELA cell was regulated quantitatively. Nek2 activation of the Wnt/β-catenin signaling pathway was dependent on the expression of downstream target genes and the Wnt/β-catenin signaling pathway itself.

Keywords: Wireless Communication, Mammal, Cell, Signal Pathway, Regulation, Protein

Introduction

A signal pathway can be defined as the phenomenon whereby a specific reaction occurring within a cell transmits a form of information from the external environment to the internal cellular milieu. This information is then interpreted by the cell, which subsequently initiates a response based on the information received (Ding et al., 2018). The signal pathway refers to a series of enzymatic reaction pathways that can transmit extracellular molecular signals into cells through the cell membrane to exert effects. These extracellular molecular signals include hormones, growth factors, cytokines, neurotransmitters and other small molecular compounds (Yoo and Lee, 2024). A variety of biochemical reaction pathways within cells are constituted by a series of distinct proteins, which facilitate a range of physiological and biochemical processes. The regulation of downstream protein activity (Including Activation or Inhibition) by upstream protein in each signal pathway is mainly achieved by adding or removing phosphate groups, thus changing the stereo conformation of downstream protein. Therefore, protein kinases and phosphatases are the main members of the signaling pathway, which can quickly change and restore the conformation of downstream proteins. This is not only a signal transduction process but also a process of gradually amplifying the external signals from the cell receptor to the final comprehensive response (Xu et al.,

2017). Receptor proteins serve to transform extracellular signals into intracellular signals, which are then amplified, dispersed and regulated by signal cascades. Ultimately, this process gives rise to a series of comprehensive cell responses, including the regulation of downstream gene expression, alterations in enzyme activity within cells, modifications to cytoskeleton configuration and changes in DNA synthesis. These changes are not all caused by one signal but also can produce different reactions through different combinations of several signals (Wang *et al.*, 2018b).

At present, there is much research on intracellular signal pathways, such as that of Nusse and Clevers (2017) tudied the regulation of the Writ/β-catenin signal pathway when Wnt and LRP5/6 were expressed in mammals. Junge et al. (2009) tudied the Fz4/LRP5 signal pathway caused by Norrin according to the fact that SPAN12 is Norrin's auxiliary receptor without Wnt dependence. The traditional research methods of cell signaling pathways included protein mutation, knockout and chemical reagent intervention. They often acted on cells for a long time. It was not known whether the mutation of the protein had other effects on its function. Protein knockout might also lead to the compensatory expression changes of other proteins. Therefore, the mutation and knockout of protein might affect the expression of other proteins. The cell function had a nonspecific effect on the accuracy of the experimental



results (Nam *et al.*, 2018). While the chemical intervention method could facilitate the rapid blocking or opening of specific signal pathways, it also revealed inherent limitations of the drug itself, including irreversible effects, high diffusion and lack of space control. Additionally, some drugs were costly and difficult to obtain, which impeded the effective temporal and spatial control of signal pathways (Wang *et al.*, 2018a).

The emergence of photogenetics has changed this situation. The physiological activities of cells can be observed and regulated by controlling the gene-encoding proteins that respond to light (Elmakias et al., 2017). In recent years, the second generations of non-channel optogenetic elements for studying cell signaling pathways have made a vigorous development, greatly enriching the means of optogenetic research. The method has numerous advantages, including non-destructive, non-invasive, high spatiotemporal resolution and high reversibility. Furthermore, it can record signal pathway molecules and their related physiological activities with high spatiotemporal resolution in combination with ultrahigh resolution micro-imaging technology. This provides a powerful solution for elucidating the mechanism of signal pathway transmission and spatiotemporal regulation (Liu, 2017). In this study, an LED light stimulation system and a wireless communication environment were constructed using optogenetics. This system utilizes CRY2/CIBN optogenetic elements to artificially control the activity of intracellular signaling proteins and enzymes, thereby achieving the goal of regulating intracellular signaling pathways.

Materials

Table 1: Experimental reagents

Subjects

In the experiment, the light control system regulates the signal transduction pathway by controlling the

activity of intracellular signaling proteins. The mammalian cells used are the human cervical cancer cell line, HeLa cells. HeLa cell is a kind of cell widely used in biological and medical research. HeLa cells exhibit the following characteristics: They can be transmitted continuously, the cell line is not subject to the limitations of aging, and they are capable of dividing indefinitely. In comparison to other cancer cells, HeLa cells demonstrate a markedly accelerated growth rate.

In the experiment, the light control system regulates the signal transduction pathway by controlling the enzyme activity in mammalian cells. The mammalian cells used in the experiment are Drosophila melanogaster cells. These cells are cultured at 60% humidity and 25°C. The hybrid of en-Gal4, tub-Gal80ts and UAS-GFP is established and cultured at 18°C for 5-7 days, then transferred to 29°C Sometimes, to enhance or weaken the expression activity of Gal4, some hybrids will be upregulated or down-regulated a little at 25°C. The Drosophila used in the experiment can be roughly divided into three categories: UAS overexpression Drosophila, UAS-RNAi, mutant Drosophila and tool Drosophila (Hajimirzaee *et al.*, 2017).

Experimental Instruments and Reagents

Main experimental instruments: Super clean table, thermo CO_2 incubator, Olympus open field microscope, self-assembled circular TIRFM microscope, Eppendorf centrifuge 5810R low-temperature freezing centrifuge, vertical plate protein electrophoresis device, water bath, mechanical shaking table, Eppendorf pipette, enzyme labeling instrument, ABI fluorescence quantitative PCR instrument, QL-861 vortex mixer and GL-802A Mini bench vacuum pump, HWS intelligent Model C constant temperature and humidity box, GE imagequant Las 4000 chemiluminescent imaging analyzer, etc. The main experimental reagents are shown in Table 1.

D	D 1	D .	D 1
Reagent name	Producer	Reagent name	Producer
DMEM	Corning, USA	DMSO	China National Pharmaceutical
FBS	GIBCO, USA	Opti-MEM	GIBCO, USA
Penicillin/Streptomycin (P/S)	Biyuntian, China	RIPA-I Cell Lysis Buffer	Biotechnology, China
0.02% EDTA trypsin	Hangyi Ke, China	Color pre-dyed protein Molecular weight make	Therrno, USA
Akt antibody	Biyuntian, China	WB second antibody(anti-rabbit or anti-mouse)	Abcam, UK
Protease inhibitor(P8340)	-	Phosphatase inhibitor (P5726/P0044)	-
Lysozyme (62971-10G-F)	-	Protease K (Tiangen)	-
Cytochalasin D (ABL43484)	-	Triton-X-100 solution	-
4% paraformaldehyde solution (PFIA)	_	-	-

Methods

LED Light Stimulation System

Design of system scheme: Using LED as the light source of the system, the LED light stimulation system is mainly composed of four parts:

- 1. Upper computer control module
- 2. Lower computer lighting module
- 3. DC power module
- 4. Bluetooth communication module

The upper computer control module is compiled by Vc ++6.0, which is mainly used to control the lower

computer Micro-Control Unit (MCU) and then to control the lighting LED array with multiple parameters. The lighting module of the lower computer is mainly composed of a 4×4 blue LED (460-465 nm) matrix and MCU. A reasonable LED array is designed to avoid the experimental error caused by uneven illumination. The DC power supply is a 220 vAc-5vDc power adapter, which supplies power to the lighting module to make the LED work normally. The Bluetooth communication module is the link between the upper computer and the lower computer. The lighting parameters set by the upper computer will reach the Bluetooth connection with the lower computer through the Bluetooth transmission connected to the upper computer. The advantage of using Bluetooth communication is that it enables wireless communication, allowing the LED array inside the incubator to be controlled outside the incubator. This avoids unnecessary trouble caused by too many wires, making the entire system simple and convenient (Hou et al., 2022).

Selection of wireless communication module: In the experiment, the cells should be placed in a constant temperature incubator for closed culture, so the data transmission mode between the upper computer and the lower computer should be considered in the design of the LED lighting system. To avoid too many data lines interfering with signal transmission, it is best to use wireless communication mode. Therefore, the module a wireless Bluetooth chip for signal transmission. The upper computer is physically connected to one end of the wireless Bluetooth chip. The lower computer is physically connected to the other end of the wireless Bluetooth chip. Thus, the physical connection between the upper computer and the lower computer has been achieved. After setting and adjusting the communication protocol and instruction format, wireless communication can be realized between them (Wang et al., 2017b).

Design of system software: The control function of the light stimulation system mainly includes setting the working state and form of the light source. The system can set the lighting parameters manually, display the current flashing mode and time of the light source and has a reasonable human-computer interface and simple operation mode. The upper computer of the light stimulation system is a software system that was developed and designed with a programming language and runs on the PC platform. The main purpose is to control the lighting mode of the lower computer light source to meet the needs of stimulating cells under different experimental conditions. Its structure is mainly divided into two modules: Body interface design and control program (El-Shafai et al., 2017). The upper computer software development system uses the development platform VC++6.0 to assist the serial port test software. The main application software used in the development process of the lower computer is

KeiluVision4 and STC_ ISP_V480, and the communication port is USB 2.0. Using the system CRY2/CIBN optogenetic element, the intracellular signal pathway is studied.

Research Scheme of Light-Controlled Adjustable P13K Signal Path

When it is known that the binding rate of CRY2/CIBN in HeLa cells is related to light intensity and the stronger the light intensity, the faster the binding rate, further experiments can be conducted by combining CRY2/CIBN elements with cell signaling pathways. The experiment includes the relationship between cell functional activity and light intensity, thereby revealing some life phenomena. In light of this premise, the subsequent research employs the components of CRY2iSH2, RFP-PHAkt and CIBN-GFP-CAAX. Among these, the regulatory subunit p85, which constitutes one of the two subunits of P13K, has been fused with CRY2 and lacks a fluorescent label. Additionally, CRY2-iSH2 is observed to exhibit diffuse cytoplasmic distribution when expressed in HeLa cells (Wang et al., 2017a). The PH domain of the N-terminal of the exogenous Akt is fused with the red fluorescent protein RFP. RFP-PHAkt is used to reflect the level of PI (3,4,5) P3 on the cell membrane. When it is expressed in HeLa, it is also in a diffuse state and distributed in the cytoplasm. It is observed that the red is evenly distributed in the cell under the fluorescence microscope. CIBN-GFP-CAAX is still a membrane localization protein with a green fluorescent label. When irradiated by a blue laser, CRY2 and CIBN will combine, and the domain of iSH2 carried by CRY2 will also move to the vicinity of the cell membrane. When iSH2 combines with the corresponding site, it will induce the endogenous P13K catalytic subunit P110 to catalyze PI (3,4) P2 on the cell membrane to generate PI (3,4,5) P3. AktPH domain is then anchored to PI (3,4,5) P3 to initiate a series of physiological responses. Therefore, when PI (3,4,5) P3 on the cell membrane increases, the number of Akt anchored to the model increases correspondingly. In HeLa cells that express RFP-PHAkt in response to blue light stimulation, the RFP-PHAkt will undergo a defined reaction, and the red fluorescence in the vicinity of the cell membrane will be intensified under TIRFM (Samimi, 2018).

Research Scheme for the Relationship between Phosphorylation of Endogenous Akt and Light Intensity

In the experiment of analyzing the relationship between endogenous Akt phosphorylation and light intensity, an LED light stimulation system is selected to stimulate the transfected cells on a large scale. In the design of light stimulation intensity, four different gradients are selected, i.e., four irradiation schemes. Option 1: 16 LED lights are completely turned off for 35 min; option 2: 16 LED lights are on for 10 sec, off for 1 min and on for 35 min; option 3: 16 LED lights are on for 1 min, off for 1 min and on for 35 min; Plan 4: 16 LED lights are fully illuminated for 35 min. The degree of blue light stimulation received by cells under different schemes is quite different, so the degree of Akt phosphorylation in corresponding cells should also be different.

After a series of operations such as cell fixation, membrane breaking, blocking and antibody incubation, the Akt phosphorylation level in cells is observed under circular TIRFM. The efficiency of liposome transfection is a limiting factor in the transfection of all cells into DNA. Therefore, when taking cell images, it is essential to distinguish between the transfected and nontransfected cells to ensure the quality of the images is not compromised. The target cell method for granulocytes is as follows: First, identify cells expressing green fluorescence of CIBN-GFP-CAAX under blue laser excitation, which represent successfully transfected cells. Second, the contour of these cells within the field of vision should be delineated. Then, observe the red fluorescent protein in the switching channel. Finally, the previously delineated area will be overlapped with the channel to determine the Akt phosphorylation level in the successfully transfected cells. At the same time, some surrounding cells are not transfected as the control group (Feng et al., 2017).

Finally, the fluorescence intensity of the transfected cells in the selected image of Image J is also used to measure the fluorescence intensity. The phosphorylation level of the heat of the transfected cells under blue light stimulation can be calculated by selecting the cells that are not transfected successfully as the blank control. The calculation method is shown in Eq. (1).

$$R_{\rm mad} = \frac{I_{\rm manan} - I_{\rm is}}{I_{\rm maxaman} - I_i} \tag{1}$$

 $I_{\rm trans}$ represents the fluorescence intensity of the successfully transfected cells in one picture. $I_{\rm untrans}$ represents the fluorescence intensity of the non-transfected cells in the same picture. $I_{\rm B}$ represents the background noise intensity in this picture. $R_{\rm akt}$ represents the relative change of Akt phosphorylation of the successfully transfected cells relative to the non-infected cells.

Then, WB was used to detect the relationship between Akt phosphorylation content and light intensity. Finally, the protein bands are analyzed using Image J software, and the gray value of each protein band is calculated and compared.

Protein Extraction

Take out the cell sample, suck the original medium with a pipette gun and wash the cell gently with PBS solution 3 times. Dry the residual solution, add the lysate

in the proportion of $10~\rm cm^2$ culture area plus $120~\rm \mu L$ lysate and put it on ice for 5-10 min. Scrape the cell off with a cell scraper, repeatedly blow the protein solution with a needle of LML syringe 8-10 times and then put the EP tube into a 4 °C centrifuge (Centrifugation at 13000 rpm) for separation. Take out the EP tube, discard the precipitate, transfer the supernatant into the new EP tube, mark it and put it into a -80 °C refrigerator for freezing.

Western Blot

According to the molecular weight of the protein to be measured, determine the concentration of the separation gel to be prepared. After the separation gel is filled, pour the concentrated gel into the upper layer and wait for 30-60 min. Put the gel into the electrophoresis tank after solidification and add the running buffer. Add maker, 1× SDS and protein samples in sequence. Set the electrophoresis time and voltage parameters. The separation gel is about 80V, 30 min, and the concentrated gel time is about 100V, 60 min. When bromo phenol orchid runs out, stop electrophoresis, transfer the membrane, remove gel and bind it to the Poly Vinyl Dene Fluoride membrane (PVDF), which is activated with methanol in advance. Clamp it into the rotating membrane trough, clamp the Transfer film buffer and set the 100 mA current. Then, the transfer time is determined based on the molecular weight of the transfer protein, usually between 2-4 h, using a PBST solution containing 5% BSA. For the blocking solution, seal the transformed membrane for 1-1.5 h. Cut out the corresponding protein strips as required. Incubate the first antibody, diluting the first antibody with the previous blocking solution in the proportion of 1:1000. Incubate the cut protein strips with the diluted antibody, storing them overnight at 4°C. Clean the protein strips with PBST the next day for 3×5 min and then dilute them with the blocking solution in the proportion of 1:10000. Second antibody: The protein strip is incubated in the dark with a diluted second antibody. After Room Temperature (RT) of 1.5-2 h, the protein strip is cleaned with PBST for 3×5 min, and then the development solution (ECL) is prepared and dropped on the strip and put into the developer for development (Dong et al., 2017).

Immunofluorescence Technique

Immunofluorescence technology is used to determine the degree of Akt phosphorylation on the cell membrane after photoactivation. PBS, 0.1% Triton-X-100 solution, and 4% polyformaldehyde solution (PFIA) are prepared. When the cell sample grows to about 70-80%, the experiment can be started. Take away the original culture medium, wash the cells in the dish gently with PBS twice, add 4% PFA to fix the cells in the dish for 10 min, then add 0.1% Triton-X-100 solution to break the membrane for 10 min. Wash the cells with PBS for 3×5 min, then use PBS with 5% BSA as the blocking solution

to seal the cells for two h. The first antibody is diluted in the proportion of 1:200, and then the cells are incubated with the first antibody after dilution. The cells are stored overnight at 4°C, washed with PBS for 3×5 min the next day, diluted with 1:200 in the closing solution and incubated in the dark for 1.5-2 h (RT). Washed with PBS for 3×5 min, then stored in the refrigerator or observed under the microscope.

Cell Phosphorylation

Phosphorylation in vitro: The enzyme and substrate are added to the prepared reaction buffer, respectively, and now 10 μ Ci [γ -32P] ATP (Perkin Elmer) is added to the reaction system. The enzyme and substrate are incubated at 30°C for two h and then boiled in a -20°C refrigerator at 94°C for 10 min.

Dephosphorylation of protein:

- 1. Recipient cells: After 3 days of transfection, the cells are resuspended and divided into two equal parts and the supernatant is removed by centrifugation
- 2. Lysed cells: The two cells are resuspended with phosphoric acid buffer and Tris buffer, respectively and incubated at 40°C at 30-40 rpm for 40-50 min
- 3. CIP treatment: After 4 °C and 12000rpm centrifugation for 12 min, take 60 μL of supernatant, add four μL CIP to the samples cracked in Tris buffer solution for 40min and then add $5\times$ SDS loading buffer

Cell Transfection

Effect Transfection

- a. Cell spreading: The full cells are resuspended and centrifuged at room temperature of 900 g for 10 min. Then, it is removed from the supernatant, cleaned with PBS again andcentrifuged to remove the supernatant. Add to the fresh culture medium and blow to make the cells fully resuspended. Finally, add to the cell culture dish, the cells after sticking to the wall account for about 60-80%
- b. Transfection: Add the plasmid to be transfected into the EC buffer and mix well. Add enhancer buffer (With a mass-to-volume ratio of 1:8 between DNA and enhancer), vortex for 10 sec immediately after addition, and let it stand for 5 min. Add effectene (According to the mass volume ratio of DNA and enhancer, 1:20). After adding, immediately warm the vortex for 10s and let it stand for 10 min. Drop the sample into the cell culture dish and shake gently to make the DNA evenly distributed

Lipofectamine Transfection

- a. Pave cells (The Same as Effect Transfection)
- b. Transfection: Add DNA into sterile PBS and mix well

The addition of Lipofectamine (1:2–3 mass/volume ratio of DNA to Lipofectamine) is added to another sterile PBS tube. Allow to stand for 5 min, taking care not to exceed 5 min. Mix the Lipofectamine with DNA in equal volume and let it stand for 20 min, taking care not to exceed 20 min. Add the mixture of Lipofectamine and DNA to the paved cells and shake gently to make the DNA evenly distributed. The whole experimental flow is shown in Figure 1.

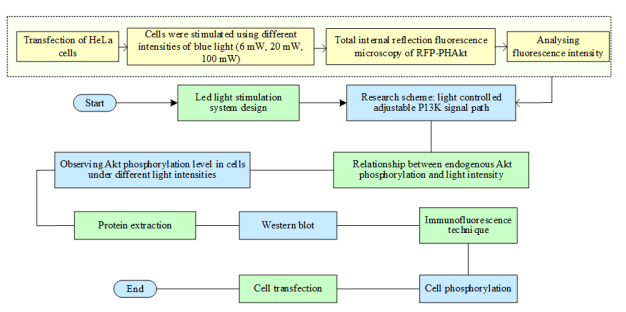


Fig. 1: Schematic diagram of the experimental process

Results

Signal Transduction Pathway Controlled by Light Control System

Research Results and Analysis of Light-Controlled Adjustable P13K Signal Path

After 15 min stimulation and photographing of HEIA cells transfected with three plasmids, a single-cell example of the change of the membrane on RFP-PHAkt over time in the living cells is shown in Figure 2.

In Figure 2, the first row and the fifth group of pictures show the dynamic changes of the upper membrane of RFP-PHAktof HeLa cell under 6mw blue light irradiation. The lower left corner shows the specific time nodes of this picture. With the time increasing to 160s, the fluorescence intensity in the cell has reached its peak. In Figure 2, the second row and the fifth group of pictures show the dynamic changes of the upper membrane of RFP-PHAkt of a HeLa cell under the blue light of 20 MW, and the fluorescence intensity reaches the peak when the time reaches 160 s. In Figure 2, the third row and the fifth group of pictures show the dynamic changes of the upper membrane of RFP-PHAkt of a HeLa cell under the blue light of 100 MW, and the fluorescence intensity reaches the peak when the time reaches 160 s.

Then, using the above data analysis method, the fluorescence intensity of 5 independent cells at each intensity is analyzed. The relative fluorescence intensity value is obtained by calculating the Standard Error (SEM) of the data by taking its average. These data are plotted as curves showing the time-dependent changes in the RFP-PH Akt membrane in live cells after 15 min of HeLa cell stimulation photography, as shown in Figure 3.

These three curves show the average of RFP-PHAkt over time in five independent cells stimulated by blue laser at 100, 20 and 6 mw and the error line is the standard error.

Figure 3 shows that under the three irradiation conditions, the intracellular fluorescence intensity will increase with the increase of time and will reach the peak value and then stop. However, the speed of reaching the peak value under each intensity will be different; that is, the dynamic characteristics of the membrane on RFP-PHAkt will be different. The data calculation is used to calculate the intracellular fluorescence intensity to reach half of the peak value under each irradiation condition. Time $T_{1/2}$ is $100 \text{ mw}_T_{-1/2} = 21.32\pm4.95 \text{ s}$, $20 \text{ mw}_T_{-1/2} = 33.71\pm5.57 \text{ s}$ and $6 \text{ mw}_T_{-1/2} = 41.32\pm9.35 \text{ s}$, respectively. $T_{1/2}$ decreases with the increase of light intensity; that is, the stronger the light intensity, the faster the film speed on RFP-PHAkt is and the shorter the time it takes to reach the peak value.

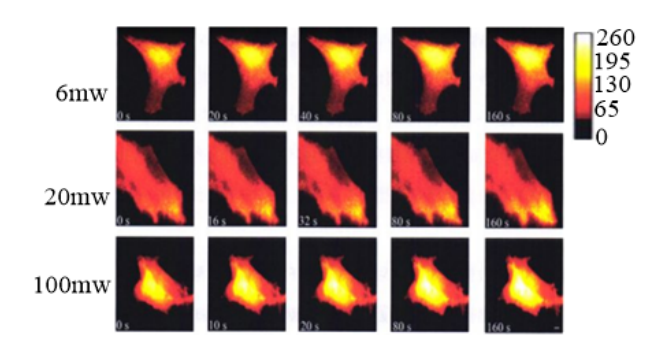


Fig. 2: Example of the change of the membrane of rfp-phakt with time under different intensities of blue light stimulation

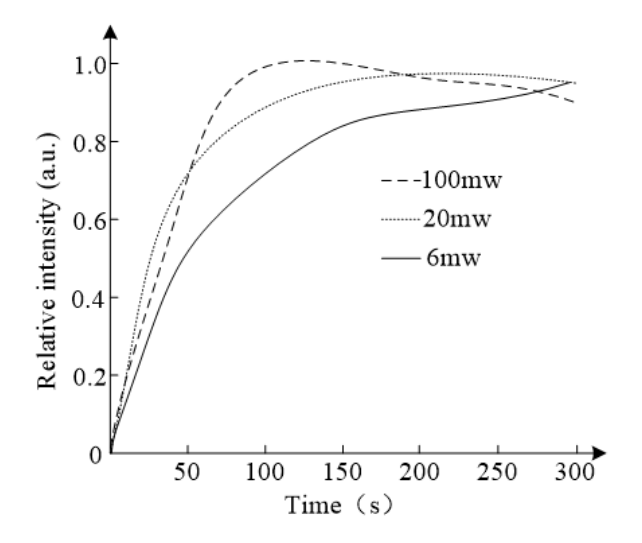


Fig. 3: Quantitative analysis of the change curve of PI(3,4,5)P3 level at any time under different light stimulation intensities (n = 5)

In this experiment, RFP-PHAkt is expressed in a foreign source. CRY2-iSH2 is combined with the

light membrane under blue excitation. Then phosphatidylinositol (PT) on the phosphorylated membrane becomes PI (3,4,5) P3 and PI (3,4,5) P3 to provide an anchor point for RFP-PHAkt. It can be inferred that when cells do not express RFP-PH Akt, the upper membrane of CRY2-iSH2 will also cause endogenous Akt to anchor to PI (3,4,5) P3 when stimulated by blue light. This will lead to the phosphorylation of Thr308 and Ser473 sites of endogenous Akt, which will then activate a variety of downstream factors such as enzymes, kinases and transcription factors through phosphorylation. These factors will subsequently regulate physiological activities.

The above experimental results indicate that the CRY2/CIBN element can achieve quantitative light regulation of the intracellular P13K signaling pathway. By controlling the intensity of light, the level of PI (3,4,5) P3 on the membrane can be regulated, providing the possibility for regulating endogenous Akt phosphorylation.

Research Results and Analysis of the Relationship between Phosphorylation of Endogenous Akt and Light Intensity

Fig. 4 is an example of the change of Akt phosphorylation degree in cells with light intensity after the cells are fixed by immunofluorescence technique under light stimulation gradient and observed by TIR and EPI (Vertical Irradiation Fluorescence). The method employs the characteristics of the immune response to amplify the level of signal for intracellular protein content step-by-step. The resulting fluorescence intensity in the fluorescent image obtained via microscopy is indicative of the protein content, with higher intensities corresponding to higher protein concentrations.

Figure 4 shows that the Akt phosphorylation level of HeLa cells transfected with CRY2-iSH2 and CIBN-GFP-CAAXwill increase when there is blue light irradiation. The Akt phosphorylation level will increase with the increase of light intensity.

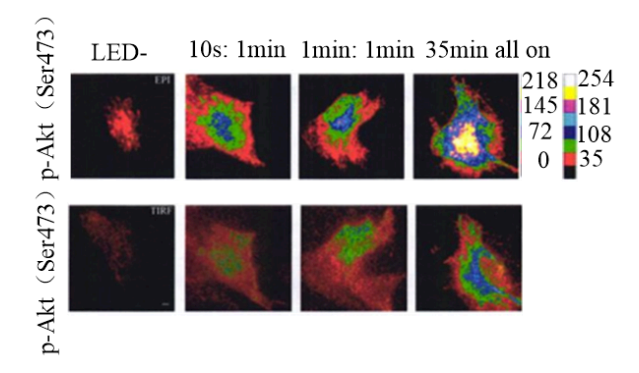


Fig. 4: Examples of Akt phosphorylation in cells under different intensities of LED stimulation in EPI and TIRF

The research scope is expanded, and 20 independent cells are selected for statistical analysis under each light stimulation condition. Figure 5 shows the measurement of fluorescence intensity corresponding to different intensities of stimulation under EPI (a) and TIRF (b) using research methods.

Figure 5 shows the ratio of the fluorescence intensity of the transfected cells to that of the non-transfected cells, that is, the ratio of the Akt phosphorylation degree of the transfected cells to that of the non-transfected cells. The Akt phosphorylation level of the transfected cells significantly increases under blue light stimulation, and with the increase of light stimulation intensity, the Akt phosphorylation level in the cells also increases.

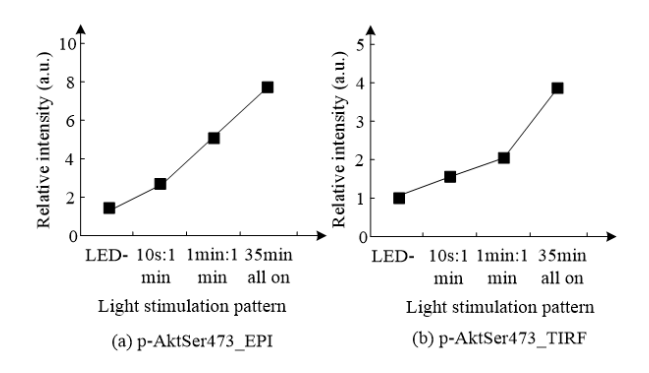


Fig. 5: Statistical analysis results of Akt phosphorylation level of multicellular under different intensities of LED stimulation under EPI and TIRF (n = 20)

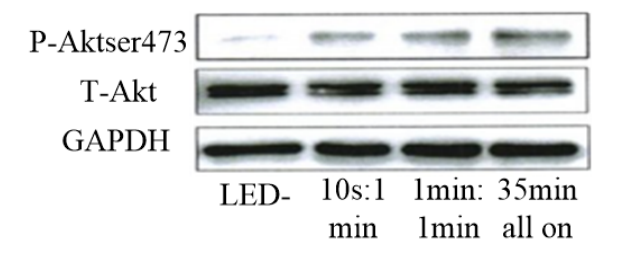


Fig. 6: Experimental results of phosphorylation of WB by Akt in cells stimulated by different intensities of LED

Then, the protein in the whole dish is extracted, and the Akt phosphorylation of the transfected cells is analyzed by Western blot. The results are shown in Figure 6. From the results of WB, the Akt phosphorylation level of cells is very low when there is no blue light stimulation. There Is no significant change in the total Akt level after blue light stimulation, but the Akt phosphorylation level in cells Is significantly increased. With the increase of light intensity, the Akt phosphorylation level in cells also increases gradually. After analyzing the fluorescence intensity data of several WB experimental bands, the results are shown in Figure 7. During the analysis, the fluorescence intensity of each sample under different conditions on the phosphorylated band is first counted, and the data are obtained by

dividing the corresponding total Akt fluorescence intensity value. The results also show that Akt phosphorylation level in cells increases with the increase of light stimulation intensity. The gray value of fluorescence bands under different stimulation conditions is analyzed by t-test, and it is found that there is a significant difference between the groups (p<0.01).

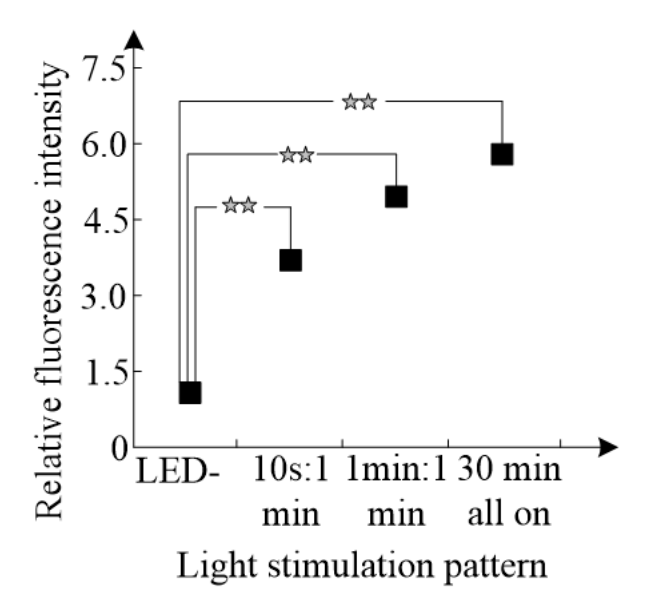


Fig. 7: Fluorescence intensity analysis results of Akt phosphorylation bands in cells stimulated by LED with different intensities (** p<0.01)

Signal Transduction Pathway Controlled by Light Control System

Activation of Wnt/β-Catenin Signaling Pathway by Nek2 Kinase Dependent Intranuclear Transcription Factor Complex

Nek2 is over-expressed on the disc of the adult wing of Drosophila larvae, and the expression of target genes downstream of the Wnt/ β -Catenin signaling pathway is observed. The results are shown in Figure 8.

From the analysis in Figure 8, Nek2 is first overexpressed using en Gal4 in the posterior intervertebral disc region of winged adults. As shown in Figure 8(a), compared with the control in Figure 8(b), overexpression Nek2 activates the expression of the downstream target genes sens (senseless) and DLL (details) of Wnt/ β -Catenin signaling pathway, as shown in Figure 8(e) and (h). In addition, overexpression of Nek2 in the middle of the wing adult disk with SalE-Gal4 can also lead to the ectopic expression of sens, as shown in Figure 8(j), indicating that overexpression of Nek2 on the wing adult disk of Drosophila larva can effectively activate Wnt/ β -Catenin signaling pathway. To verify whether Nek2 directly regulates the expression of wg and affects the Wnt/ β -Catenin signaling pathway, the

expression of wg in overexpression of Nek2 is observed. Moreover, because wg itself is not the target gene of the signaling pathway, it can also be used as a control for the overexpression of Nek2, which affects transcription. It is found that the expression of wg is not affected by overexpression of Nek2, as shown in Figure 8(c), which indicates that Nek2 regulates the Wnt/β-Catenin signal pathway rather than the expression of the wg gene itself. At the same time, knock down Nek2 on the adult disk of Drosophila wings to observe whether it is necessary for normal development. Knockdown Nek2 has no significant effect on gene expression downstream of the Wnt/β-Catenin signaling pathway (data not shown), which suggests that Nek2 may have functional redundancy genes. The transcription of the downstream target gene of the Wnt/β-Catenin signaling pathway is regulated by the complex of arm and pan. Therefore, further observation is conducted on whether the activation of target genes sens and DLL in the Wnt/B-Catenin signaling pathway by Nek2 was also regulated by this complex. When Nek2 is overexpressed and the pan is knocked down, the expression of sens and DLL is inhibited, as shown in Figure 8(f) and (i). In addition, Pygo can bind to arm through Lgs in the nucleus and upregulate the transcription of downstream target genes. Combined with these two experiments, Nek2 can activate the Wnt/β-Catenin signaling pathway and upregulate the expression of downstream target genes depending on the transcription factor complex.

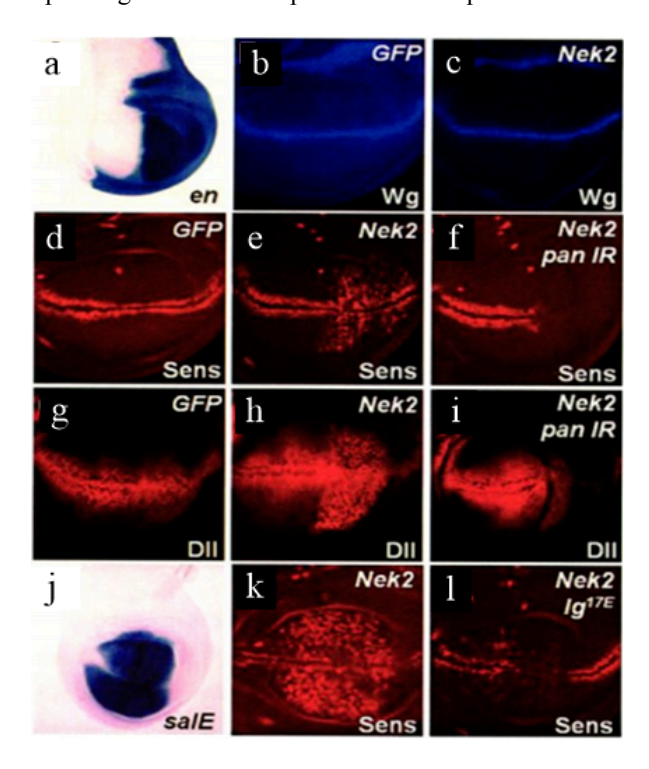


Fig. 8: Activation of Wnt/β-Catenin signal by overexpression of Nek2 depends on the intranuclear transcription factor complex

Up-Regulation of Wnt/β-Catenin Signaling Pathway at N-terminus of Phosphorylated Dsh by Nek2

The results of the up-regulation of Wnt/ β -Catenin signaling pathway activity at the N-terminus of phosphorylated Dshby Nek2 are shown in Figure 9.

1-340 at the N-terminal of the Dsh can slightly activate the wf reporter, but compared with the fulllength Dsh, its activity is very low, as shown in Figure 9(c). However, both of them can effectively activate Wnt/β-Catenin signaling pathway by CO transformation with Nek2, which shows that the activity of Dsh1-340 is greatly improved after being phosphorylated by Nek2, as shown in Figure 9(e). To further analyze the function of Nek2 phosphorylated Dsh, a number of different truncated mutations based on different N-terminal domains of Dsh is further constructed and their expression levels in Kc cells are detected, as shown in Figure 9(a) and (d). The activation of the Wnt/β-Catenin signaling pathway by Nek2 phosphorylation of the Dsh N-terminal requires neither basic nor proline-rich modules, but Dix and PDZ domains, both of which are indispensable. A truncated mutation contains only DIX and PDZ domains. Dsh (1-92)+(248-340) can still activate the wf-reporter very effectively after being phosphorylated by Nek2, as shown in Figure 9(b) and (e). Therefore, it is believed that the binding of Dsh's PDZ domain to Nek2 leads to Nek2 phosphorylating Dsh's DIX domain. Phosphorylated Dsh activity significantly increases, thereby upregulating the expression of downstream target genes in the Wnt/β-Catenin signaling pathway.

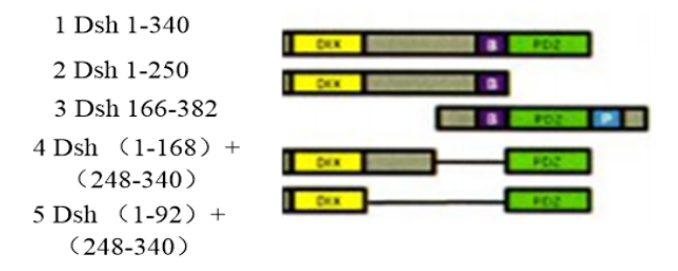
Discussion

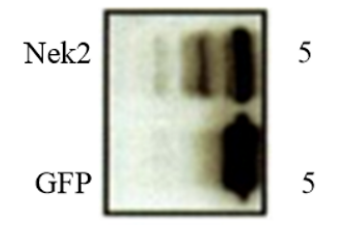
This article uses the CRY2/CIBN pair of photogenerating elements, combined with circular TIRFM micro imaging, to study the signal protein activating enzyme activity signaling pathway in cells that can be controlled by adjustable light.

In this study, the light control system regulates the signal transduction pathway by modulating the activity of intracellular signaling proteins. By leveraging the nonfunctional dynamic characteristics of CRY2/CIBN, we investigated how different intensities of blue light stimulation affect the levels of PI (3,4,5) P3 on the membrane, which is controlled by light-regulated PI3K activity. The results showed that the PI (3,4,5) P3 level on the membrane was directly proportional to the light intensity, and the higher the light intensity, the greater the effect. Then, an LED light stimulation system was used to stimulate the transfected cells on a large scale. The relationship between phosphorylation of Akt, a downstream signal protein of P13K and light intensity was studied by combining if and WB technology (Sarkar et al., 2018). These schemes were used to stimulate the cells. The difference in Akt phosphorylation level between the transfected and non-transfected cells was

analyzed by if and WB detection (Zhang and Ai, 2017). The results showed that light not only increased the level of PI (3,4,5) P3 on the cell membrane but also increased the phosphorylation of Akt. When the intensity of light stimulation was changed, the degree of Akt

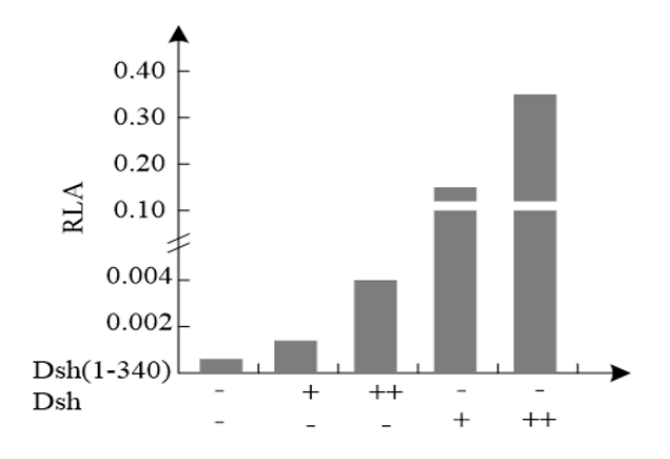
phosphorylation in cells would also change. Through this study, the light-controlled adjustable PI3K/PI (3,4,5) P3 signaling pathway system was investigated, achieving precise light-controlled regulation of mammalian cell signaling pathway activation (Gulbahar, 2017).

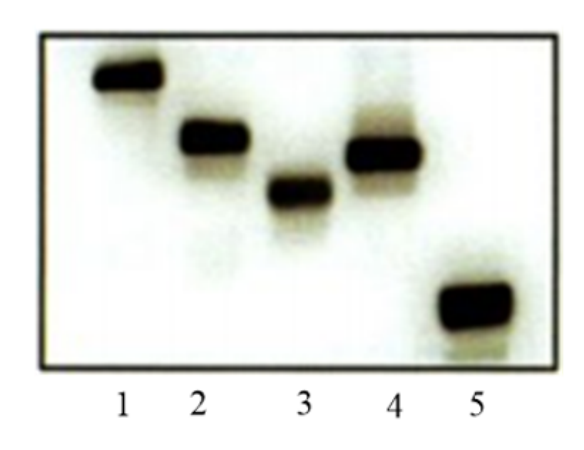




(a): Further subdivision of the N-terminal of Dsh constructs different truncation mutations

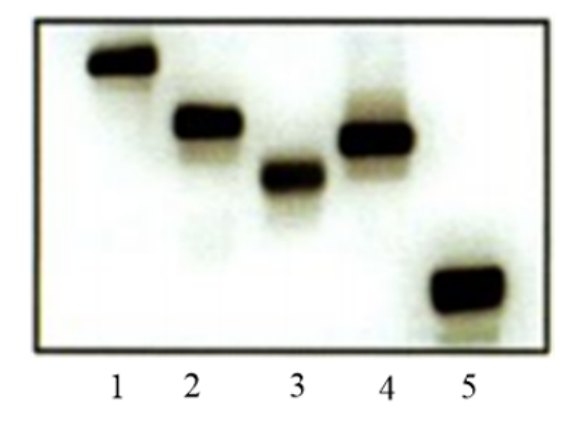
(b): Dsh(1-92)+(248-340) is phosphorylated by Nek2Dsh





(c): Low efficacy and full length of Dsh 1-340 in activating WF reporter

(d): Western blot to detect the expression level of N-terminal truncated mutation in Kc cells



(e): Effect of co-expression of different N terminal truncated mutations of Nek2 and Dsh on the activity of WF reporter

Fig. 9: Results of up-regulation of Wnt/β-Catenin signaling pathway activity at N-terminus of phosphorylated Dsh by Nek2

In the study of the signal transduction pathway controlled by the light control system, the non-functional dynamics of CRY2/CIBN were used. The overexpression library was established by integrating 655 CD (coding domain sequence) sequences of cell growth and cell cycle genes under the UAS into the 86F of chromosome

3 of Drosophila melanogaster. It was found that Nek2 interacted with the Wnt/β-Catenin signaling pathway by using this library combined with hierarchical clustering, string and phenotype observation under a sensitive background. As shown in Figure 7, Nek2 relied on the activation of the signaling pathway by the transcription

factor complex in the nucleus. Genetic epistasis was used to determine the interaction between Nek2 and Dsh, and Nek2 was located upstream of Dsh. By constructing a series of Dsh truncation mutations, it was found that the N-terminus of Dsh can be phosphorylated by Nek2. The N-terminus of Dsh phosphorylated by Nek2 could activate Dsh, upregulate the Wnt/β-Catenin signaling pathway and promote the transcription of downstream target genes, as shown in Figure 8. By analyzing the effect of Nek2 on Dsh protein levels and the impact of Nek2 or Dsh overexpression on wf reporter genes, the study suggests that Nek2 phosphorylation of Dsh should be a dynamic process. When the activity of the Wnt/β-Catenin signaling pathway is low, the activity of the Dsh N-terminus phosphorylated by Nek2 increases, thereby rapidly activating the Wnt signaling pathway. When the activity reaches a certain level, Dsh's activity is phosphorylated by Nek2. In addition, Nek2 can reduce the protein stability and accelerate the degradation of Dsh to prevent the over-activation of the signal pathway, which is a protective mechanism (Li et al., 2025).

Conclusion

To study the regulation of signal pathways in mammalian cells in a wireless communication environment, an LED light stimulation system is designed and built under the conditions of low cost, low power consumption, convenience and stability. This study designed a data communication module to solve the problem of teaching data transmission between the upper computer and the lower computer, avoiding excessive data line interference in signal transmission. It controlled the lighting mode of the LED matrix by setting different parameters. A Bluetooth module was used to connect the upper computer and the lower computer to achieve wireless communication. By using the system CRY2/CIBN light genetic software, the regulation of PI3K/Akt signal pathway by the change of signal protein activity in HeLa cells and Wnt/β-Catenin signal pathway by Nek2 kinase in Drosophila melanogaster cells were studied.

Although this study has achieved some results, there are still several issues that need to be addressed. For example, the design and construction of LED light stimulation systems can be further optimized to enhance their stability. Additionally, the selection of controllable parameters should be expanded to accommodate a broader range of light stimulation experiments. Moreover, the number of light bulbs should be increased to meet the requirements for larger radius culture dishes. The objective of conducting rapid drug screening was accomplished through the integration of the experiment and the drug screening process.

Funding Information

The authors have not received any financial support or funding to report.

Ethics

Research experiments conducted in this article with animals were approved by the Ethical Committee and responsible authorities of our research organization (s), following all guidelines, regulations, and legal and ethical standards as required for animals.

References

- Elmakias. D. Bykhovsky, D., Arnon, S. (2017). Air Turbulence Effects on Performance of Optical Wireless Communication with Crosstalk in Server Backplane. Chinese Optics Letters, 15(2), 020602-020606. https://doi.org/10.3788/col201715.020602
- Ding, J., Wang, J., Jin, H., Xia, T., Cheng, Y., Wu, J., & Han, X. (2018). Microcystin-LR Reduces the Synthesis of Gonadotropin-Releasing Hormone by Activating Multiple Signaling Pathways Resulting in Decrease of Testosterone in Mice. Science of The *Total Environment*, 643, 496–506.

https://doi.org/10.1016/j.scitotenv.2018.06.123

- Dong, G., Teng, Y., Jiang, X., Guo, D., & Li, Qiang. (2017). Deterministic Dendritic Cell Algorithm for Online Detection of Botnet. Journal of Jilin University Science Edition.
- El-Shafai, W., El-Rabaie, S., El-Halawany, M., & Abd El-Samie, F. E. (2017). Enhancement of Wireless 3D Video Communication Using Color-Plus-Depth Error Restoration Algorithms and Bayesian Kalman Filtering. Wireless Personal Communications, 97(1), 245-268. https://doi.org/10.1007/s11277-017-4503-x
- Feng, Q., Zhang, Y., Li, C., Dou, Z., & Wang, J. (2017). Anomaly Detection of Spectrum in Wireless Communication Via Deep Auto-Encoders. The Journal of Supercomputing, 73(7), 3161–3178. https://doi.org/10.1007/s11227-017-2017-7
- Gulbahar, B. (2017). A Communication Theoretical Analysis of Multiple-Access Channel Capacity in Magneto-Inductive Wireless Networks. *IEEE* Transactions on Communications, 65(6), 2594– 2607. https://doi.org/10.1109/tcomm.2017.2669995
- Hajimirzaee, P., Fathi, M., & Qader, N. N. (2017). Quality of Service Aware Traffic Scheduling in Wireless Smart Grid Communication. Telecommunication Systems, 66(2), 233–242. https://doi.org/10.1007/s11235-017-0285-4
- Hou, B., Yi, L., Li, C., Zhao, H., Zhang, R., Zhou, B., & Liu, X. (2022). An interactive mouthguard based on mechanoluminescence-powered optical fibre sensors for bite-controlled device operation. Nature Electronics, 5(10), 682-693.

https://doi.org/10.1038/s41928-022-00841-8

Junge, H. J., Yang, S., Burton, J. B., Paes, K., Shu, X., French, D. M., Costa, M., Rice, D. S., & Ye, W. (2009). TSPAN12 Regulates Retinal Vascular Development by Promoting Norrin- but Not Wnt-Induced FZD4/β-Catenin Signaling. Cell, 139(2), 299–311. https://doi.org/10.1016/j.cell.2009.07.048

- Li, Z., Li, X., Xia, H., Wang, Y., & Wei, N. (2025). NEK2 promotes the progression of osteoarthritis by stabilizing ATF2 through phosphorylation at Ser-112 and inhibiting autophagy. *International Immunopharmacology*, *146*, 113833. https://doi.org/10.1016/j.intimp.2024.113833
- Liu, B. (2017). 4.8-Gbit/s Broadband Wireless Communication Link at Radio Frequency using Orbital Angular Momentum and Polarisation Multiplexing. *Electronics Letters*, 53(18), 1248–1250. https://doi.org/10.1049/el.2017.1699
- Nam, I., Lee, S., & Kim, D. (2018). Advanced Monopole Antenna with a Wide Beamwidth for the Assessment of Outdoor 5G Wireless Communication Environments. *Microwave and Optical Technology Letters*, 60(9), 2096–2101. https://doi.org/10.1002/mop.31313
- Nusse, R., & Clevers, H. (2017). Wnt/β-Catenin Signaling, Disease, and Emerging Therapeutic Modalities. *Cell*, *169*(6), 985–999. https://doi.org/10.1016/j.cell.2017.05.016
- Samimi, H. (2018). Generalised Statistical Distribution for Turbulence-Induced Fading in Wireless Optical Communication Systems. *IET Optoelectronics*, *12*(3), 136–143.
 - https://doi.org/10.1049/iet-opt.2017.0007
- Sarkar, T. K., Chen, H., Salazar-Palma, M., & Zhu, M.-D. (2018). Physics-Based Modeling of Experimental Data Encountered in Cellular Wireless Communication. *IEEE Transactions on Antennas and Propagation*, 66(12), 6673–6682. https://doi.org/10.1109/tap.2018.2878366
- Wang, C., Feng, X., & Ma, H. (2017a). Effects of Spatial Frequencies Distributions on the Phase Synchronization. *Journal of China Academy of Electronics and Information Technology*, 12, 394–399

- Wang, J., Fang, R., & Sun, W. (2017b). QoS Modeling of Wireless Sensor Networks in Smart Distribution Grid Communication. *Wireless Personal Communications*, 95(4), 4477–4495. https://doi.org/10.1007/s11277-017-4096-4
- Wang, T., Liu, S., & Ge, L. (2018a). Design of High-Speed Wireless Communication Receiver in Parallel DC/DC System. *Journal of Power Supply*, 16, 166–170.
- Wang, X., Jiang, H., Tang, T., & Zhao, H. (2018b). The QoS Indicators Analysis of Integrated EUHT Wireless Communication System Based on Urban Rail Transit in High-Speed Scenario. *Wireless Communications and Mobile Computing*, 2018(1), 2359810. https://doi.org/10.1155/2018/2359810
- Xu, Q., Ren, P., Song, H., & Du, Q. (2017). Security-Aware Waveforms for Enhancing Wireless Communications Privacy in Cyber-Physical Systems via Multipath Receptions. *IEEE Internet* of Things Journal, 4(6), 1924–1933. https://doi.org/10.1109/jiot.2017.2684221
- Yoo, S., & Lee, H. J. (2024). Spheroid-Hydrogel-Integrated Biomimetic System: A New Frontier in Advanced Three-Dimensional Cell Culture Technology. *Cells Tissues Organs*, 1–20. https://doi.org/10.1159/000541416
- Zhang, R., & Ai, B. (2017). A Channel Estimation Method for OFDM Based Wireless Communication System in High Speed Environment. *Wireless Personal Communications*, 94(3), 909–926. https://doi.org/10.1007/s11277-016-3657-2